SUPPORTING INFORMATION FOR

Light-induced Changes in Magnetism in a Coordination Polymer Heterostructure, $Rb_{0.24}Co[Fe(CN)_6]_{0.74}@K_{0.10}Co[Cr(CN)_6]_{0.70}\cdot nH_2O$ and the Role of the Shell Thickness on the Properties of both Core and Shell

Olivia N. Risset [a], *Pedro A. Quintero* [b], *Tatiana V. Brinzari* [b], *Matthew J. Andrus* [a],

Michael W. Lufaso [c], *Mark W. Meisel* [b,*] *and Daniel R. Talham* [a,*]

[a] Department of Chemistry, University of Florida, Gainesville, FL 32611-7200, USA

[b] Department of Physics and the National High Magnetic Field Laboratory, University of Florida, Gainesville, FL 32611-8440, USA

[c] Department of Chemistry, University of North Florida, Jacksonville, FL 32224-7699, USA

This supporting information contains: **(1)** EDS line scans on RbCoFe@KCoCr core@shell particles; **(2)** TEM image of RbCoFe cores; **(3)** Size dispersion for RbCoFe cores and RbCoFe@KCoCr heterostructures; **(4)** Predicted particle size for the RbCoFe@KCoCr structures; **(5)** FT-IR spectra for for RbCoFe cores and RbCoFe@KCoCr heterostructures; **(6)** PXRD patterns at 300 K for RbCoFe cores and RbCoFe@KCoCr heterostructures; **(7)** PXRD patterns at 160 K for RbCoFe cores and RbCoFe@KCoCr heterostructures; **(8)** Refined lattice constants at 300 K and 160 K for RbCoFe cores and RbCoFe@KCoCr heterostructures; **(9)** PXRD patterns stacked as a function of temperature, from 300 K to 160K, for the core@shell samples **1** and **3**; **(10)** Simulation of χT vs. T values in the CTIST region (300 – 150 K) and detailed analysis; and **(11)** Magnetization vs. Field at T = 5 K for **1**, **2**, and **3** in the dark and light state, after irradiation at 5 K.

[*] Corresponding authors: talham@chem.ufl.edu; meisel@phys.ufl.edu

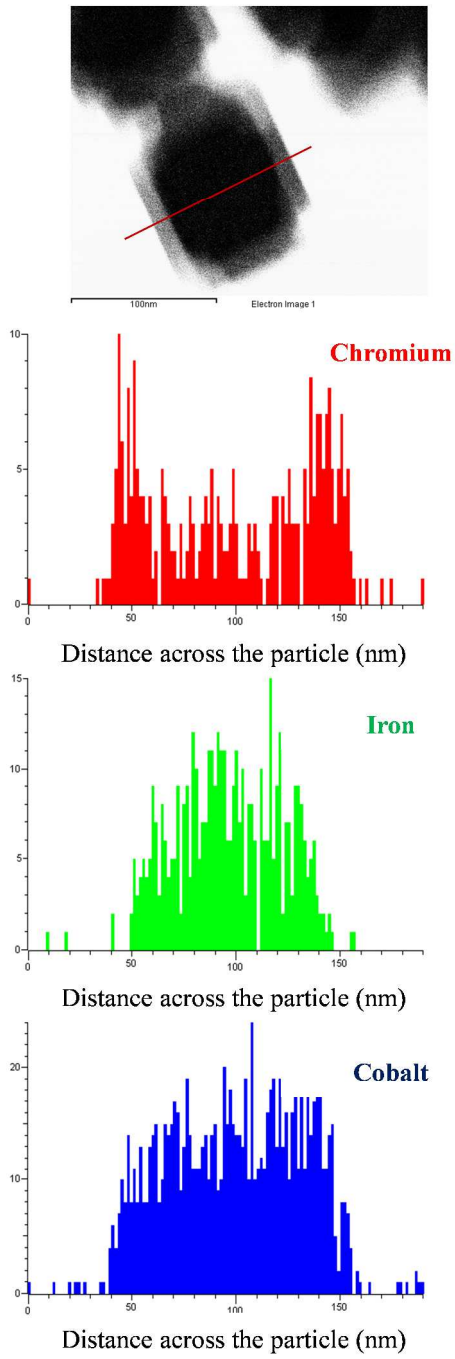

Figure S1. EDS line scans on an individual RbCoFe@KCoCr core@shell particles with a shell thickness of 35 nm. Data represent the counts for each element detected as a function of the position of the electron beam across the particle. EDS line scans confirm the chemical assignments and the segregation between core and shell materials within the particle.

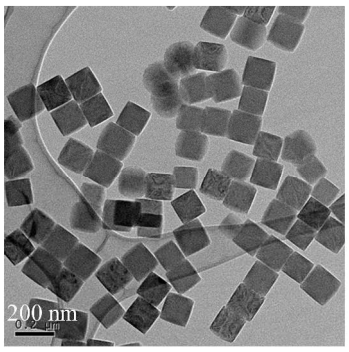

Figure S2. TEM image of RbCoFe cores shows a well-defined cubic shape and are nearly uniform in size, 135 ± 12 nm. Scale bar is 200 nm.

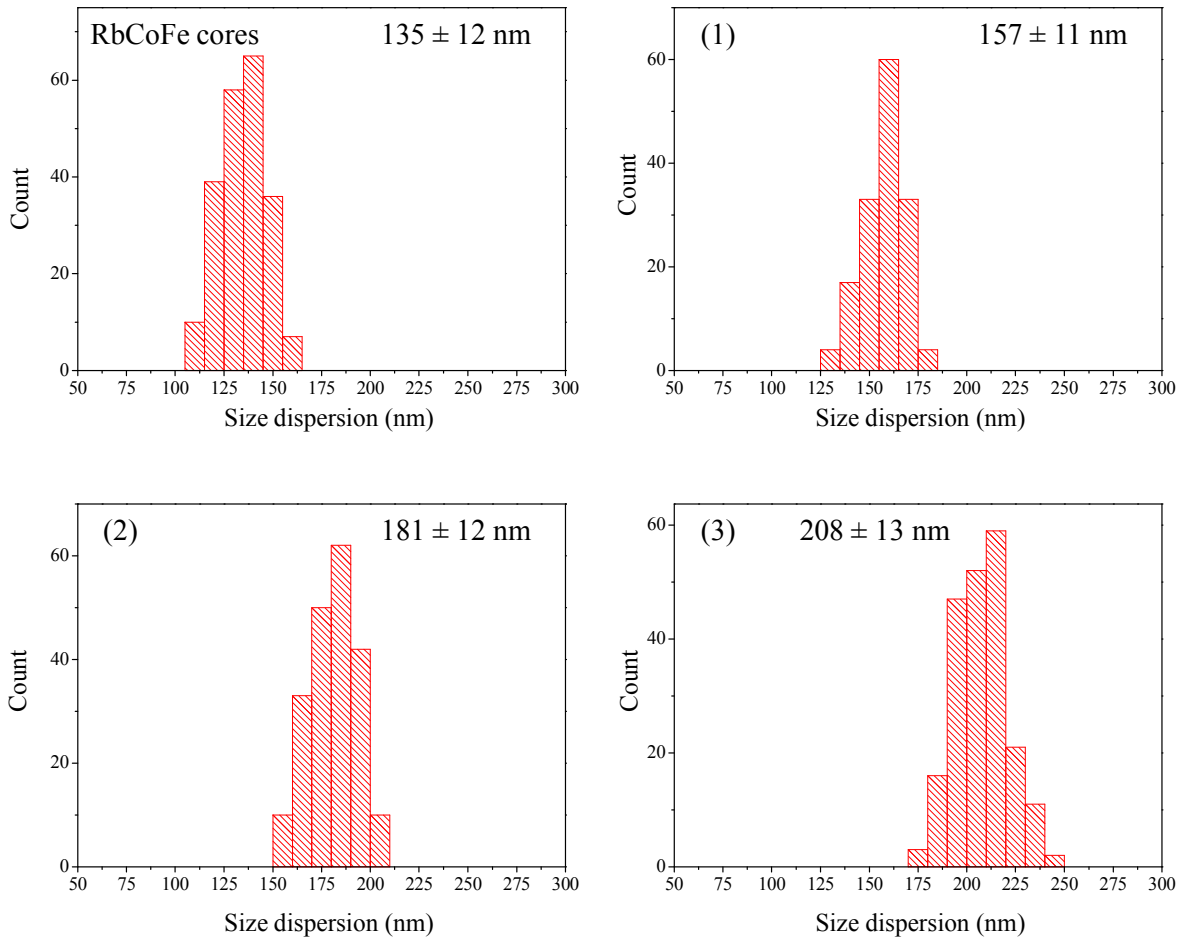

Figure S3. Size dispersion for RbCoFe cores, **1**, **2** and **3**. The methods used to determine the mean size values and the corresponding uncertainties are described in the main paper.

	1	**2**	**3**
n_{core} (mmol)	0.40	0.30	0.22
n_{shell} (mmol)	0.20	0.14	0.14
a_c: average core size (nm)	135	157	181
$a_{c\text{-}s}$: predicted size (nm)	155	178	213
measured size (nm)	157 ± 11	181 ± 12	208 ± 13

Table S4. Predicted size vs. measured size for RbCoFe@KCoCr heterostructures **1**, **2** and **3**. As detailed by Catala et al.,[†] the equation $a_{c\text{-}s} = a_c\ (1 + n_{shell}/n_{core})^{1/3}$ provides predictions of the size of a core@shell particle ($a_{c\text{-}s}$) when the size of the core (a_c), the number of moles of core material (n_{core}) and the number of moles of shell material (n_{shell}) are known. Below, a schema shows the lengths $a_{c\text{-}s}$ and (a_c).

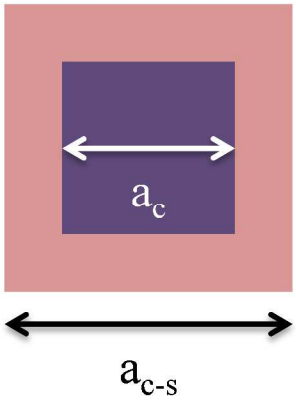

[†] Catala, L.; Brinzei, D.; Prado, Y.; Gloter, A.; Stephan, O.; Rogez, G.; Mallah, T. *Angew. Chem., Int. Ed.* **2009**, *48*, 183-187.

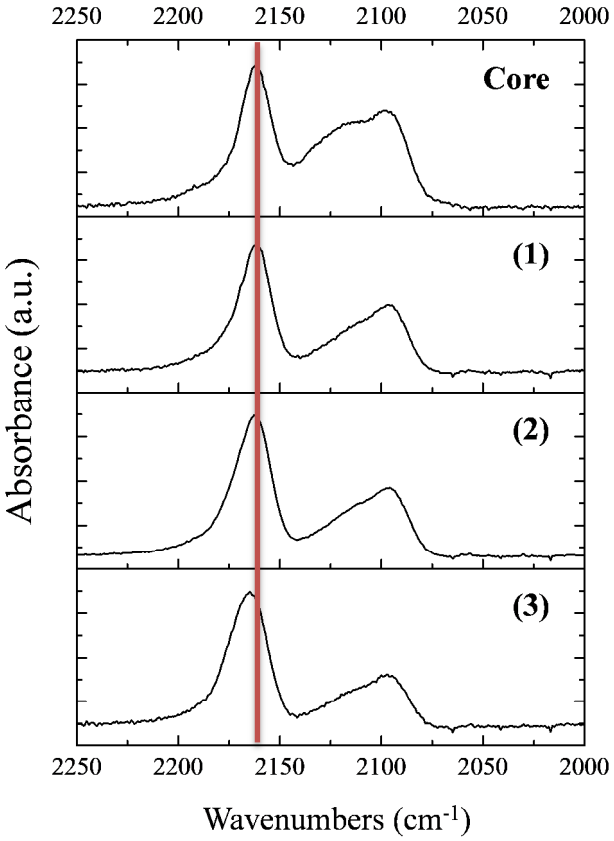

Figure S5. FT-IR spectra for RbCoFe cores and RbCoFe@KCoCr core@shell particles **1**, **2** and **3**. The red line indicates the position of the peak corresponding to Co^{II}-NC-Fe^{III} (HS). As the shell thickness increases, this peak shifts and becomes asymmetric due to the emergence of a peak around 2170 cm^{-1} consistent with KCoCr.

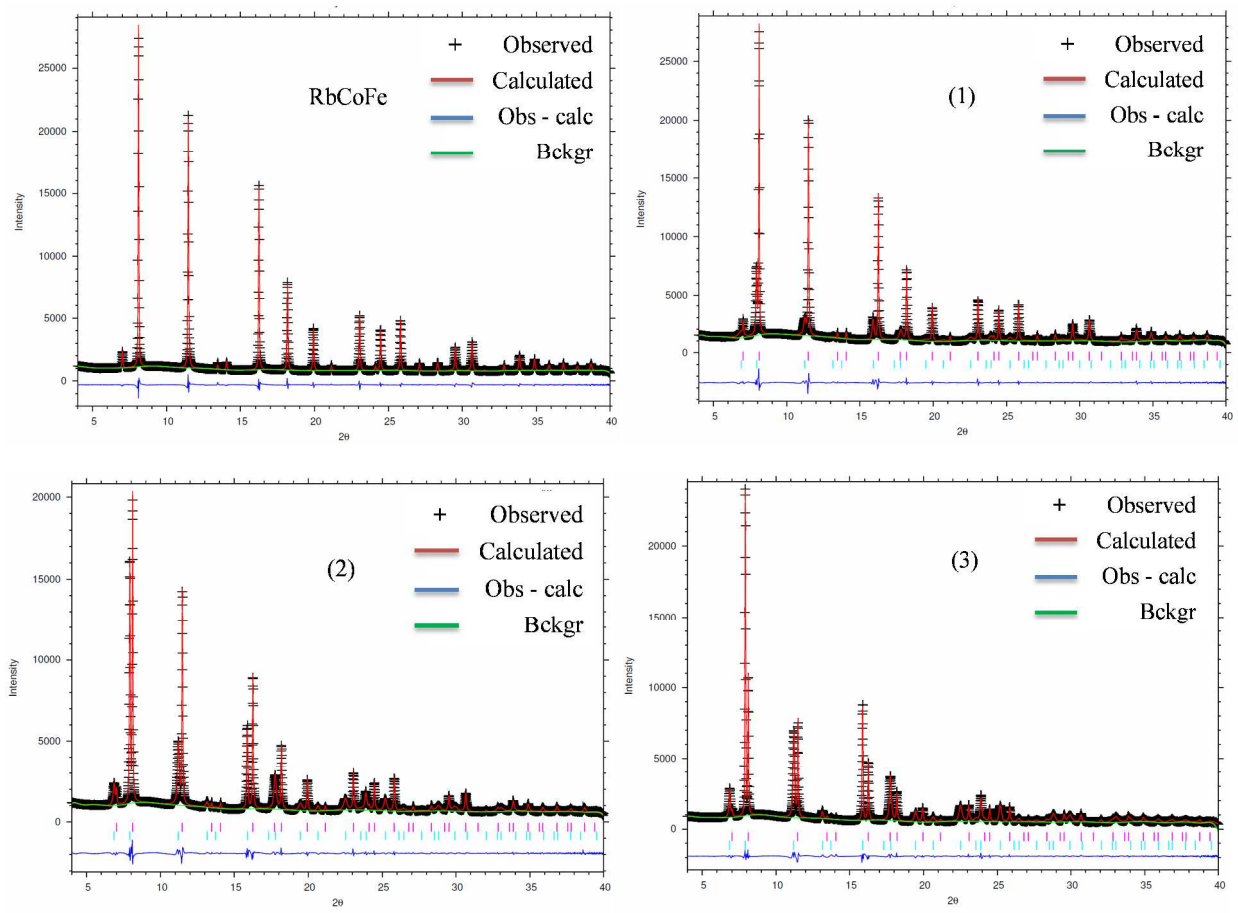

Figure S6. PXRD patterns at 300 K for RbCoFe cores and RbCoFe@KCoCr **1** (t = 11 nm), **2** (t = 23 nm) and **3** (t = 37 nm), indexed in the space group *Fm-3m* (No. 225) and fitted using Le Bail method and refined lattice constants. For the heterostructures, the set of peaks at higher angles correspond to the RbCoFe core while the one at lower angles are attributed to the KCoCr shell.

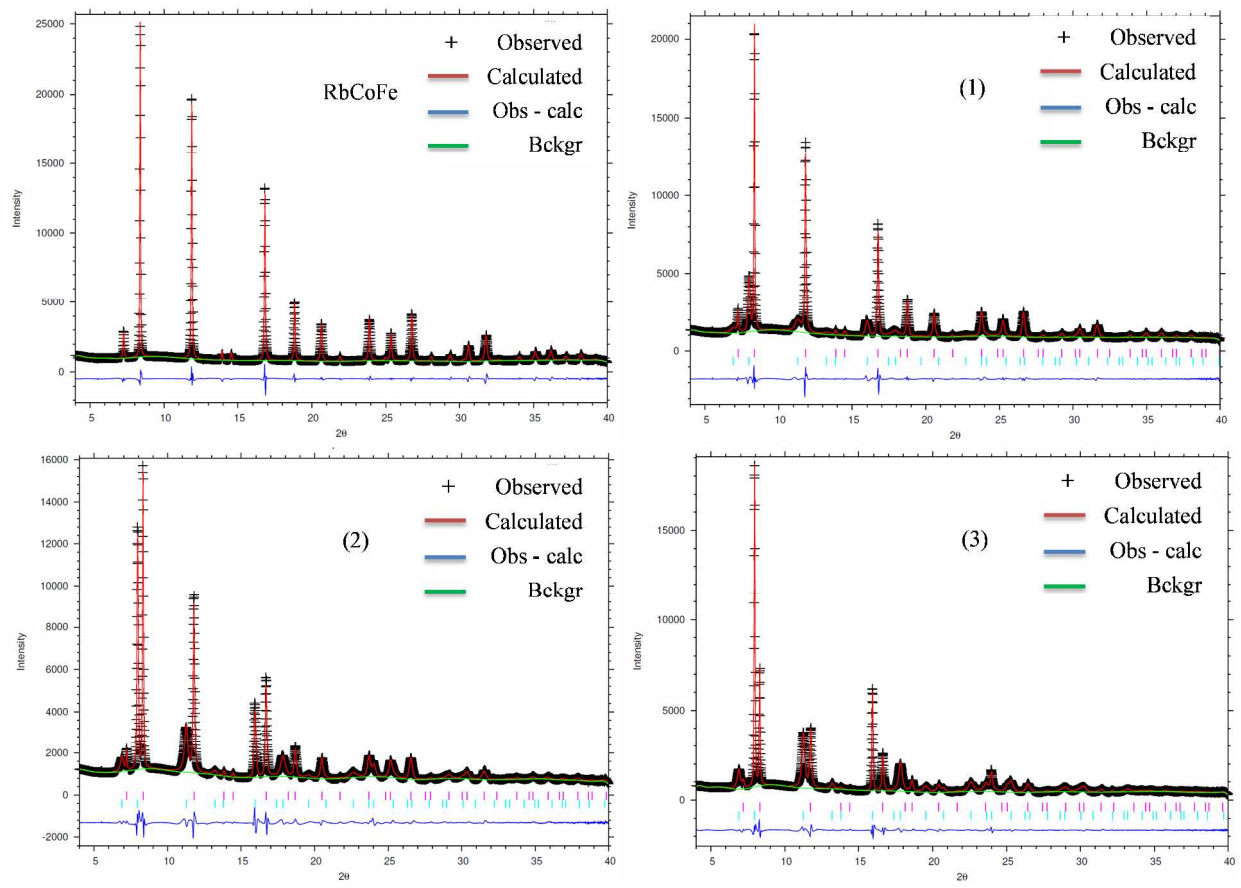

Figure S7. PXRD patterns at 160 K for RbCoFe cores and RbCoFe@KCoCr **1** (t = 11 nm), **2** (t = 23 nm) and **3** (t = 37 nm), indexed in the space group *Fm-3m* (No. 225) and fitted using Le Bail method. For the heterostructures, the set of peaks at higher angles correspond to the RbCoFe core while the one at lower angles are attributed to the KCoCr shell.

		11 nm		23 nm		37 nm	
	RbCoFe	RbCoFe	KCoCr	RbCoFe	KCoCr	RbCoFe	KCoCr
Lattice parameter *a* at 300 K (Å)	10.30348(3)	10.30188(4)	10.5309(3)	10.30492(5)	10.5508(1)	10.29832(8)	10.55055(7)
Lattice parameter *a* at 160 K (Å)	9.94490(5)	9.98994(7)	10.4455(5)	10.0290(1)	10.4931(2)	10.0719(2)	10.5112(1)
Δ*a* (RbCoFe) (Å)	0.359	0.312		0.276		0.226	
Δ*a* (KCoCr) (Å)			0.085		0.058		0.039

Table S8. Refined lattice constants at 300 K and 160 K for RbCoFe cores and RbCoFe@KCoCr **1** (*t* = 11 nm), **2** (*t* = 23 nm) and **3** (*t* = 37 nm), indexed in the space group *Fm-3m* (No. 225) and fitted using Le Bail method. Δ*a* represents the difference in cell parameters between 300 K and 160 K.

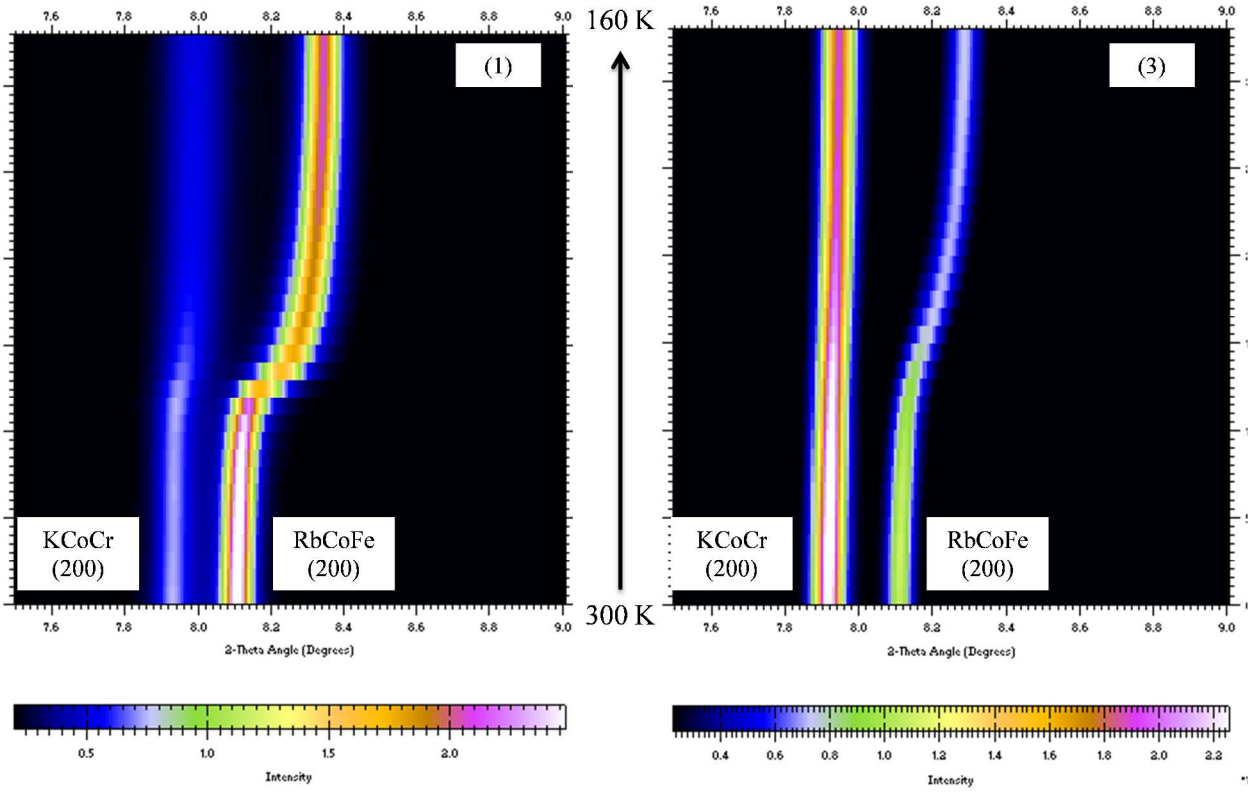

Figure S9. PXRD patterns collected every 5 K and stacked as a function of temperature, from 300 K to 160K at a cooling rate of 2 K/min, for the RbCoFe@KCoCr samples **1** and **3**.

CTIST analysis in the three core@shell samples

In this section, the low field (100 G) magnetic response is analyzed in the high temperature region of 150 K < T < 300 K. The results clearly indicate the CTIST in the CoFe-PBA is complete for the bare cores and for the three core@shell samples.

SI.1.1 Complete CTIST for the bare cores

The analysis begins by realizing that the CTIST is complete for the bare cores, as suggested from the values of the magnetic data and the absence of magnetic ordering at low temperature (T ≈ 20 K). More explicitly, the χT value at room temperature of 2.9 (Fig. S10) is in agreement with the value expected from the formula $Rb_{0.24}Co^{II}[Fe^{III}(CN)_6]_{0.74}\cdot 3.5\ H_2O$ and the isolated values of high-spin Co^{II} (S=3/2 , g ≈ 2.3) and low-spin Fe^{III} (S =1/2 , g ≈ 2.7) (Li, D. et al., *J. Am. Chem. Soc.* **2008**, *130*, 252-258) yield, in cgs units per spin when using $\chi T = \frac{1}{8}g^2 S(S+1)$,

$$\frac{1}{8}(2.3^2)(\frac{3}{2})(\frac{5}{2})+\frac{1}{8}(2.7^2)(\frac{1}{2})(\frac{3}{2})0.74 = 2.98 \quad . \tag{5}$$

In addition, the χT value at 150 K of 0.8 (Fig. S10) is consistent with the formula $Rb_{0.24}Co^{II}{}_{0.26}Co^{III}{}_{0.74}[Fe^{II}(CN)_6]_{0.74}\cdot 3.5\ H_2O$, where all the Co^{II}-Fe^{III} pairs in the (HS state) have transitioned to Co^{III}-Fe^{II} (LS state), namely

$$\frac{1}{8}(2.3^2)(\frac{3}{2}\frac{5}{2})0.26 = 0.64 \quad . \tag{6}$$

Finally, the last piece of evidence for the completeness of the transition is the paramagnetic behavior of the bare cores down to 5 K, indicating the absence of antiferromagnetic coupled Co^{II}-Fe^{III} pairs, that give raise to a ferrimagnetic transition with $T_c \approx$ 20 K.

SI.1.2 Complete CTIST for the three core@shell samples

If there were no interactions between the core and the shell, and they both behave independently, the magnetic data of the system would be just the superposition of the core and shell responses,which can be written as

$$(\chi T)_{core@shell} = \frac{n_{core}}{n_{core@shell}}(\chi T)_{core} + (1-\frac{n_{core}}{n_{core@shell}})(\chi T)_{shell} \quad , \tag{7}$$

where n_x, the the number of moles of the x-component (core, shell or core@shell), can be calculated from the equation $n_x = mass_x/MW_x$. The ratios between the masses can be calculated from the EDS data, and the MW are known (see experimental section). In Figure S10, the data for the core, the shell, and the three core@shells are shown, along with the results of the simulations corresponding to equation (7). It is noteworthy that the room temperature values of

the simulated and actual data differ in less than 0.04 emu K/mol, suggesting that, at this high temperature, the cores and shells behave as two independent magnetic components, and the cores are in the HS state. At 150 K, the χT values of the measured data are are slightly lower than those predicted by equation (7), (Fig. S10), and this observation suggests that the cores have undergone a complete transition to the LS state. The small difference between the actual and simulated values at 150 K is most likely linked to changes in the g-values coming from the strain induced during the CTIST. Finally, in the intermediate temperature region (200-275 K), the actual and simulated data differ due to the large synergy CTIST event in the system as extensively discussed in the main text. Modeling the influence of this synergy on the magneto-lattice cooperativity is beyond the scope of the present discussion, and the simplier cooperative effects through the CTIST transistion, which have been modeled, are also not included.[‡,§,**]

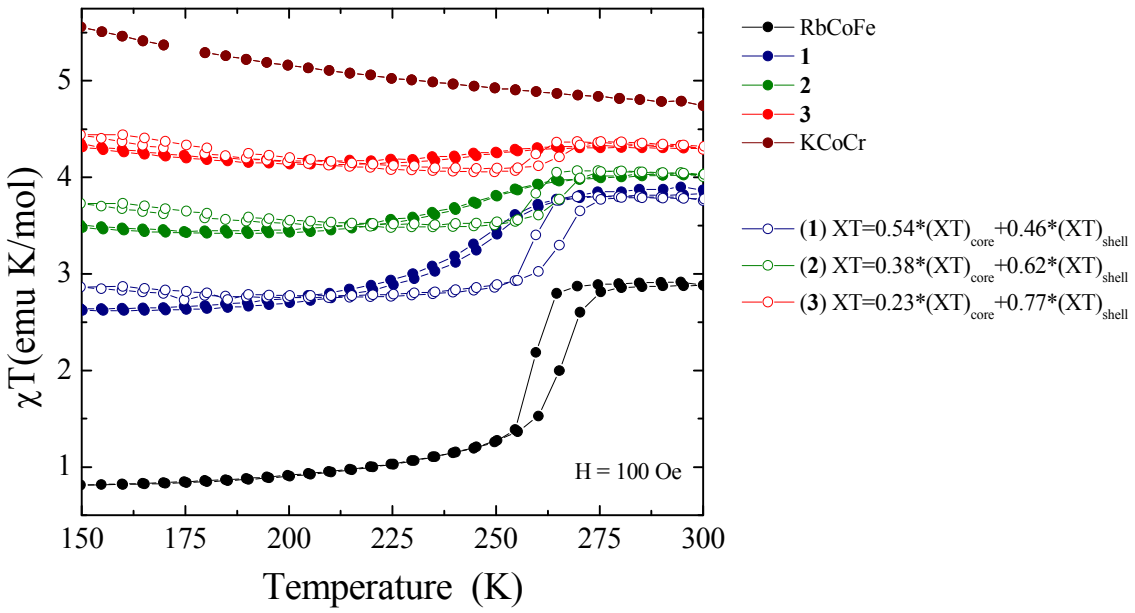

Figure S10. Simulated χT vs. T data are based on two assumptions: (i) the RbCoFe core is in the high spin state at 300 K; (ii) the RbCoFe core fully converts to the LS state at 150 K. Simulated χT vs. T data (empty dots) at 300 K match well with the experimental data (filled dots) which confirms that the core is in the high spin state, consistent with IR and XRD data. At 150 K, the experimental χT value is lower than the simulated value for all three core@shell heterostructures which indicates a complete transition of the core to the LS state.

[‡] Hôo, B.; Boukheddaden, K.; Varret, F. *Eur. Phys. J. B* **2000**, *17*, 449.
[§] Pajerowski, D. M.; Ravel, B.; Li, C. H.; Dumont, M. F.; Talham, D. R. *Chem. Mater.* **2014**, *26*, 2586.
[**] Konishi, Y.; Tokoro, H.; Nishino, M.; Miyashita, S. *Phys. Rev. Lett.* **2008**, *100*, 067206.

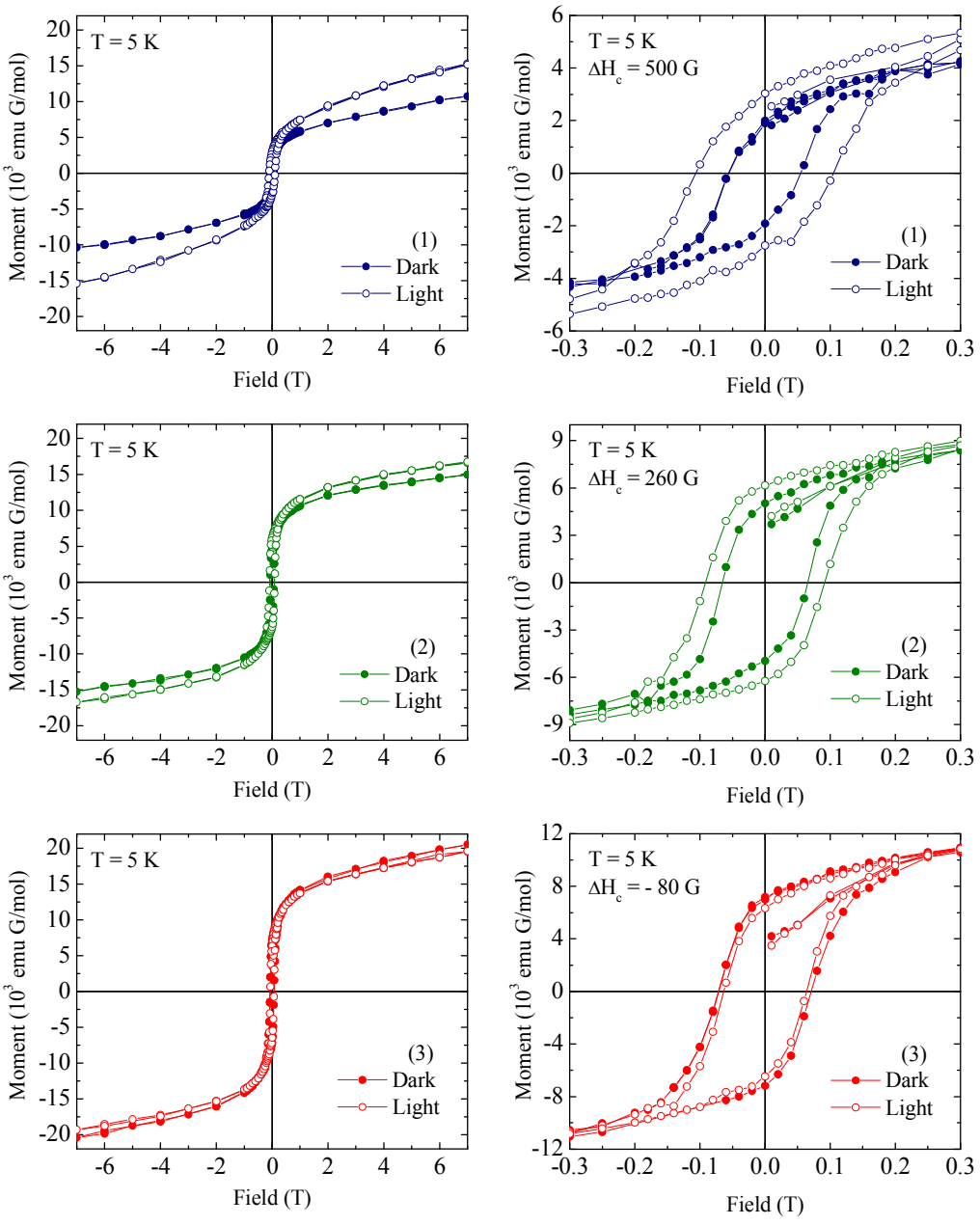

Figure S11. Magnetization vs. Field at T = 5 K for **1** (top), **2** (center), and **3** (bottom) in the dark state (filled dots) and light state, after irradiation at 5 K (open dots). The plots on the left show the whole field sweep while the plots on the right display only the low field region.